



iJRASET

International Journal For Research in
Applied Science and Engineering Technology



INTERNATIONAL JOURNAL FOR RESEARCH

IN APPLIED SCIENCE & ENGINEERING TECHNOLOGY

Volume: 9 Issue: III Month of publication: March 2021

DOI: <https://doi.org/10.22214/ijraset.2021.33165>

www.ijraset.com

Call:  08813907089

E-mail ID: ijraset@gmail.com

Performance Evaluation of an Airfoil Fabricated through Additive Manufacturing, using Simulation and Experimental Techniques

M. Krishna¹, S. Raghav², S. Raghuraman³, Siva Chidambaram P⁴, T. Pannerselva⁵m

^{1,2}Undergraduates, ³ Professor, ⁴Ph.D. Scholar, ⁵Senior Assistant Professor, School of Mechanical Engineering, SASTRA University, Thanjavur-613401, India

Abstract: The purpose of this research work is to implement the use of additive manufacturing techniques for fabricating bodies, where the functional performance of the body predominantly depends on the nature of the surface, like an aerofoil. The additive manufacturing technique employed in this research work is fused deposition modeling, FDM process is generally used to fabricate thermoplastic parts, it deploys molten polymer filament to generate multiple sliced cross-sections of the desired part. To carry out the objectives of this paper a NACA 6 series aerofoil is chosen because of its ability to produce maximum lift coefficient, and an advanced 3D printing material, PLA+ (High-grade Polylactic acid), is chosen based on its mechanical properties. The 3D printed aerofoil is tested for its performance by measuring the values of lift and drag coefficients under varying experimental parameters. The analysis report is evaluated using both software simulation and wind tunnel experiments under the same operating parameters. The results obtained for PLA+ aerofoil are compared with a similar aerofoil fabricated, using ABS material, by the same process of manufacturing. The variations in performance between the two aerofoils can be addressed based choice of material and its surface roughness after 3D printing. From this study, we conclude that surface characteristics play a vital role in deciding the performance of an aerofoil. The surface roughness of the additively manufactured high-grade PLA aerofoil is around $18 \times 10^{-6}m$. Therefore the corresponding values of coefficient of lift and drag are 0.115m/s and 0.048m/s respectively. Whereas the surface roughness value for ABS is around $20 \times 10^{-6}m$ and its corresponding maximum coefficient of lift and drag are 0.09 and 0.048 m/s.

Keywords: 3DPrinting, Aerofoil, FDM, High-grade PLA, ABS, Coefficients of lift and drag, Surface roughness.

I. INTRODUCTION

Additive Manufacturing (AM), also known as 3D printing, is a layer by layer fabrication of 3D objects from a digital model. It is being used for the production of series of components for the most demanding applications[1]. The use of additive manufacturing technology is in increasing demand in various industries such as Aerospace, Automotive, transportation and also in medical industries because of their ability to produce complex parts(Near-net shape) and also zero wastage of materials, unlike conventional manufacturing[4]. Various metal alloys and composites are the materials used for producing components. They are used in producing parts in gas turbine engines such as vanes, stators, seals, rotors, and even geometrically complex parts such as aerofoils, dusks and diffusers[2,3]. Some of the techniques used for producing complex shapes are as follows:

- A. Selective laser sintering,
- B. Selective laser melting,
- C. Fused deposition modeling
- D. Stereolithography,
- E. Fused filament fabrication and
- F. Laminated object manufacturing[5].

The advantages of using this technique over conventional methods are increased design freedom, lightweight structures, near-net-shape capability, less production time and economic low volume production[8].

Creating Finite Element Analysis (FEA) module for analyzing of main AM processes is considered as a smart developing step to model and simulate of AM technology.

Fused deposition modeling (FDM), a leading Rapid Prototyping technique, accomplishes the layer-by-layer build by depositing a material extruded through a nozzle in a raster pattern (i.e., in a pattern that is composed of parallel lines) in each layer[6]. FDM works by taking a part designed by a computer-aided design (CAD) model exported as a stereolithography (STL) file and uploaded into a slicer program. The slicer program cross-sections the model into individual layers of a specified height and converts the desired height and other settings into G-Code to be X-Y read by the printer. The printer reads the G-Code, heats up a liquefier to the desired temperature to melt the polymer filament of choice, and begins extruding the material. These filaments are fed through the heated liquefier by two drive wheels where the filament is then melted and extruded through a nozzle onto the build platform.

The heating and extrusion of the filament to the specified diameter is all contained within the extrusion head which moves in the plane depositing material on the build platform. After each layer is finished the build platform moves down a specified layer height and the process repeats for the next cross-sectioned layer until the part is completed[7].

Additive manufacturing in aerospace sector is crucial since it provides numerous advantages. Thermoplastic polymers like ABS, PLA, PLA+(high-grade PLA) are being widely used for additive manufacturing for their application in aerospace industries. One such example is use of thermoplastic polymers is in matrix phase in polymer matrix composites as the reinforcement medium. They are widely preferred over thermosetting polymers due to their high hydraulic stability and non-toxic nature. Various works on PMC using thermoplastics as matrix phase with fiber reinforcements. They observed considerable good results with the use of the thermoplastics[9,10,11].

Also current research of thermoplastics in nanocomposites is gaining huge interest since the speed of processing can be increased to achieve effective design process[12].

Aerofoil component performance is equally important in this wide sector. Previous research works have been carried out on designing and printing of airfoil by additive manufacturing with ABS as material. Properties such as surface roughness and dimensional accuracy play an important role in determining the performance of an airfoil. A good material which tends to provide excellent smoothness and accuracy is a great advantage for this industry. This paper attempts to build a NACA series airfoil with high heat grade PLA material which is seen to show better results when compared to ABS material

II. EXPERIMENT

A. Selection of Material

The material used to 3D print the model of the aerofoil is high-grade PLA otherwise known as PLA+. High-grade PLA (PLA+) is chosen as an alternative to ABS material for the fabrication. The reason for choosing this material is because of its high strength, high rigidity, and stronger layer bond.

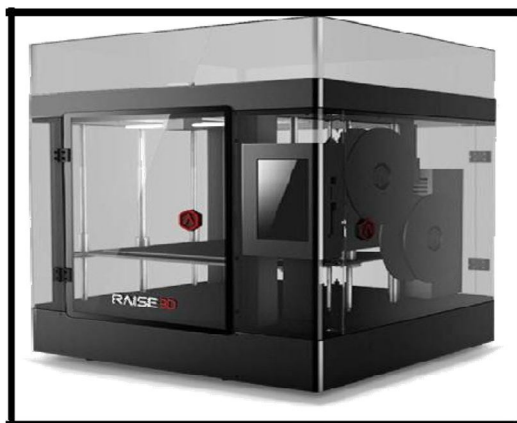


Figure 1 Raise 3D printer.

When focusing on the quality of the part, it has sharper details (corners, surfaces) when compared to part produces with ABS as material[13]. Also, lower warping, better odor and fewer particle emissions are some of the distinctive features of choosing this material. Table 2 shows the comparative study of PLA+, PLA and ABS material according to ASTM standard. Figure 3 shows the variation of normalized mechanical strength (%) for both ABS and high-grade PLA. From both table and graph, one can see that the properties of high heat grade PLA material is superior compared to standard PLA and ABS material.

Table 1: Comparative Data points for High Heat Grade PLA vs Standard PLA vs ABS (Data according to ASTM E8 specifications.)

Properties	HighHeatGrade PLA	StandardPLA	ABS
High Distortion Temp(HDT)	144°C	55°C	85°C
Flexural modulus,	646,000 Psi	555,000 Psi	298,000 Psi
Flexural strength,	18,300 Psi	12,000 Psi	8500 Psi
Tensile Yield Strength,	9500 Psi	8700 Psi	5900 Psi

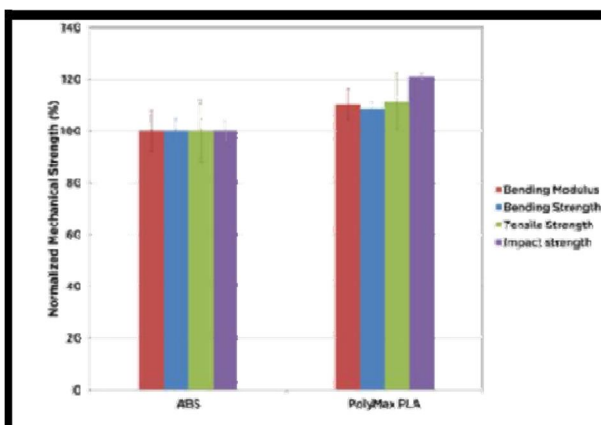


Figure2: Shows the variation of Normalized mechanical strength (%) for both ABS and high-grade PLA.

B. Aerofoil CAD modeling

The performance of the aircraft depends on the design parameters of the aerofoil taken into consideration[14]. A NACA 6 series aerofoil is chosen for CAD modeling, i.e. NACA 652215. The 6 series aerofoils were developed to maximize the region over which the airflow remains laminar, which in fact reduces the drag over a small range of lift coefficient, however the performance of an additively manufactured 6 series NACA aerofoil is yet to be evaluated, the purpose of this research work is to bridge the above research gap. The advantages of this type of aerofoil is that it has the capacity to produce high maximum lift coefficient, and a very low drag over a small range of operating conditions, albeit found in majority of the applications in the aviation field like piston-powered fighters, business jets, jet trainers etc., it may have some drawbacks with respect to high pitching moment, and poor stall behavior. The specifications for the aerofoil are provided in table 2.

Table 2: Show:s specifications of the aerofoil.

<i>Aerofoil Specifications</i>	
NACA Series	652215
Wingspan	0.25m
Chord length	0.20m
Wingspan area	0.05m ²
Mean Thickness	0.045m

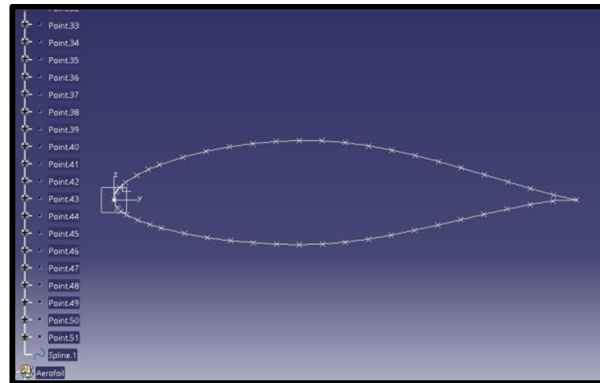


Figure3 (a):Illustrating NACA652215-Aerofoil spline

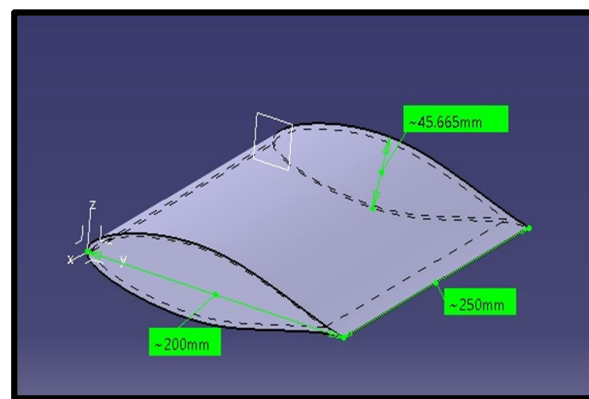


Figure 3 (b):Aerofoil part body

The part file generated in design environment of CATIA (See figures 3(a) and 3(b).) is imported in an STL Rapid-prototyping workbench. This STL file is supplied as an input to the 3D printer. Figure 4 shows the aerofoil at the culmination of 3D printing.



Figure 4: 3Dprinted Aerofoil

C. Method of Printing

A stereolithographic file of the aerofoil is imported to 3D printer's respective slicer software to create the G-code used to print each specimen type. FDM process is used for carrying out the printing of airfoil. These filaments are fed through the heated liquefier by two drive wheels where the filament is then melted and extruded through a nozzle onto the build platform.

The heating and extrusion of the filament to the specified diameter is all contained within the extrusion head which moves in the x-y plane depositing material on the build platform. RAISE3D printer is used for printing the airfoil. The printing was carried out at an extrusion speed of 150mm/s with 2-headed nozzle, having a diameter of 0.4mm and a filament diameter of 1.75mm. The printing temperature is about 300°C.

D. Simulation Studies

The simulation analysis is carried out using the ANSYS fluent workbench. The aerofoil part-file is imported to ANSYS Fluent workbench and the required angle of attack is set. A boundary layer is also imported in the same environment to measure the flow regimes and pressure forces acting over the aerofoil.

Table 3: Showing Initial Boundary conditions.

Conditions	Values
Inlet velocity	5m/s*
Wall boundary	Specified shear.
SolvingMethod	Implicit Method
Turbulence model	K-Epsilon
Turbulence Intensity	5%

*the angle of attack and velocity are changed and the performance of the aerofoil is calculated for each condition

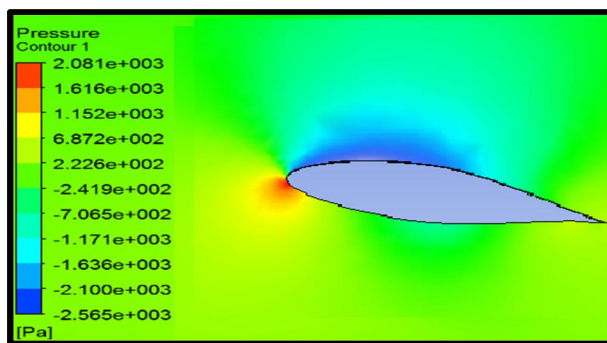


Figure 5: Pressure distributions (Pa) over the aerofoil

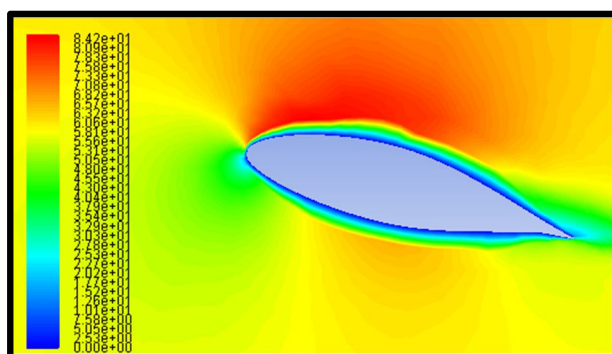


Figure6: Velocity contour (m/s)over the aerofoil

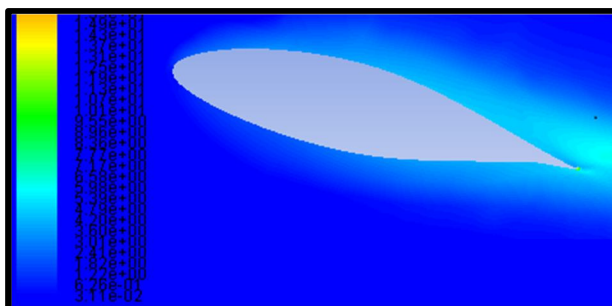


Figure 7: Turbulence intensity (%) around the aerofoil

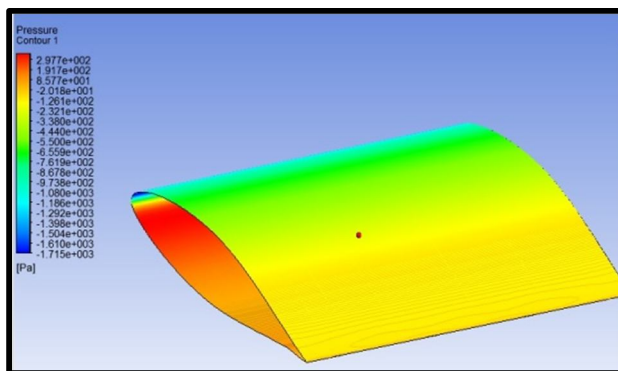


Figure 8:Aerofoil under maximum pressure loading

The tabulation for the lift force, drag force, the coefficient of lift, the coefficient of drag with respect to change in angle of attack (AOA) with variation in velocity is shown in the tables below.

Table4:Variation of Coefficient of lift with Angle of attack at various speeds

		<i>Coefficient of lift</i>				
<i>AOA(α)</i>		-6	0	6	12	18
<i>SPEED(m/s)</i>						
5		-0.435	0.176	0.706	1.237	1.420
10		-0.450	0.180	0.689	1.280	1.506
15		-0.433	0.163	0.604	1.282	1.570
20		-0.436	0.181	0.695	1.320	1.550
25		-0.471	0.181	0.696	1.339	1.572
30		-0.440	0.165	0.788	1.305	1.623
45		-0.442	0.165	0.801	1.313	1.638
60		-0.448	0.161	0.697	1.319	1.650

Table5:Variation of Coefficient of drag with Angle of attack at various speeds

		<i>Coefficient of Drag</i>				
<i>AOA(α)</i>		-6	0	6	12	18
<i>SPEED(m/s)</i>						
5		0.036	0.031	0.046	0.070	0.126
10		0.031	0.013	0.042	0.061	0.110
15		0.023	0.021	0.048	0.063	0.104
20		0.024	0.022	0.040	0.056	0.106
25		0.026	0.019	0.039	0.055	0.104
30		0.021	0.018	0.026	0.058	0.094
45		0.020	0.015	0.026	0.056	0.091
60		0.020	0.014	0.037	0.057	0.906

Table6: Variation of lift Force with Angle of attack at various speeds

	<i>Lift force (N)</i>				
<i>AOA(α)</i>					
<i>SPEED(m/s)</i>	-6	0	6	12	18
5	-0.330	0.135	0.541	0.940	1.091
10	-1.380	0.552	2.112	3.930	4.614
15	-2.985	1.127	4.167	8.836	10.810
20	-5.340	2.216	8.519	16.180	19.060
25	-9.020	3.460	13.340	25.650	30.110
30	-12.152	4.556	21.730	35.994	44.760
45	-27.428	10.246	49.712	81.487	101.920
60	-49.456	17.740	76.939	145.511	181.820

Table7: Variation of Drag force with Angle of attack at various speeds

	<i>Drag force(N)</i>				
<i>AOA(α)</i>					
<i>SPEED(m/s)</i>	-6	0	6	12	18
5	0.017	0.012	0.027	0.042	0.086
10	0.060	0.042	0.102	0.150	0.324
15	0.102	0.082	0.273	0.357	0.650
20	0.210	0.171	0.403	0.567	1.190
25	0.331	0.239	0.628	0.876	1.840
30	0.392	0.299	0.547	1.364	2.410
45	0.864	0.631	1.28	3.035	5.320
60	1.606	1.042	5.754	5.446	9.370

E. Wind Tunnel Experiment

The performance of the additively manufactured aerofoil is then evaluated using a wind tunnel setup, see Figure 9.

A C- Clamp is used for mounting the aerofoil in the test section of the wind tunnel. The Clamping setup is shown in figure 10. The clamp is then mounted in the wind tunnel test section and the required angle of attack is set. Initially, the angle of attack was set at -6° and the performance of aerofoil is measured for airspeed from 4.2m/s till 35m/s, subsequently measuring the values of lift force, drag force and the shear force acting over the aerofoil. These forces are measured with the help of a sensor affixed to the C-clamp holding the aerofoil. Once the behavior of the aerofoil at -6° is measured, the same experiment is carried out for the next series of AOA from 0° to 18° and the corresponding values of forces are noted and tabulated.



Figure 9: Wind tunnel



Figure 10: Clamping of aerofoil using a C-Clamp

Calculations are carried out to compute the values of coefficient of lift (C_L) and coefficient of drag(C_D) for each angle of attack and air velocity.

To find the values for corresponding C_L the formula used is

$$C_L = L / (0.5 * \rho * S * v^2) \tag{1}$$

Where L represents the lift force in Newton, ρ is the density of air at sea level conditions (constant value 1.2253kg/m^3) and S represents the wingspan area 0.05m^2 . Similarly, the values for the corresponding C_L are obtained by using the formula is

$$C_D = D / (0.5 * \rho * S * v^2) \tag{2}$$

Where D represents the value of drag force in Newton, and the other parameters represent the same quantity as stated above.

The experimental results are tabulated, given below, and graphs are plotted between the results obtained in the simulation and the experimental report, However for the angle of attack other than 0° , the experimental flow analysis on the aerofoil was restricted to an airspeed between 30-35m/s as the turbulence developed within the test section of the wind tunnel was strong enough to tilt the mounted lightweight aerofoil.

Table8: Performance evaluation for AOA= (- 6°)

S.No	Velocity (m/s)	Lift (N)	Drag (N)	Coefficient of Lift (N)	Coefficient of Drag	Speed Rpm	Side Shear
1	4.2	-0.02	0.01	0.0370	0.0185	169	-0.01
2	8.4	-0.07	0.04	0.0324	0.0185	322	-0.02
3	15.1	-0.20	0.10	0.0286	0.0143	484	-0.03
4	22.3	-0.44	0.20	0.0289	0.0131	703	-0.05
5	27	-0.65	0.30	0.0291	0.0134	843	-0.05
6	31.2	-1.10	0.41	0.0369	0.0137	910	-0.06

Table9: Performance evaluation for AOA 0°

S.No	Velocity (m/s)	Lift (N)	Drag (N)	Coefficient of Lift (N)	Coefficient of Drag	Speed Rpm	Side Shear
1	4.2	0	0.01	0	0.018	157	0.01
2	10.9	0.04	0.06	0.011	0.016	350	0.01
3	14.3	0.13	0.09	0.207	0.014	450	0.01
4	25.7	0.4	0.21	0.198	0.0104	700	0
5	30	0.52	0.27	0.0189	0.0098	803	0
6	35	0.75	0.36	0.0200	0.0096	920	-0.01
7	38	0.90	0.44	0.0203	0.0099	1015	-0.01
8	40	0.99	0.49	0.0202	0.0100	1058	-0.01
9	45.1	1.31	0.63	0.0210	0.0101	1203	-0.02
10	50.2	1.58	0.75	0.0205	0.0097	1311	-0.03
11	54	1.89	0.87	0.0212	0.0097	1412	-0.03

Table10:Performance evaluation for AOA 6°

S.No	Velocity (m/s)	Lift (N)	Drag (N)	Coefficient of Lift (N)	Coefficient of Drag	Speed Rpm	Side Shear
1	4.2	0.04	0.01	0.0740	0.0185	146	0
2	11.2	0.34	0.07	0.0885	0.0182	353	-0.01
3	17.7	0.73	0.14	0.0760	0.0146	502	-0.01
4	21.1	1.10	0.20	0.0806	0.0147	600	-0.01
5	26.1	1.60	0.30	0.0767	0.0144	721	-0.02
6	30.3	2.15	0.42	0.0764	0.0149	821	-0.02

Table 11:Performance evaluation for AOA 12°

S.No	Velocity (m/s)	Lift (N)	Drag (N)	Coefficient of Lift (N)	Coefficient of Drag	Speed Rpm	Side Shear
1	4.2	0.05	0.02	0.0925	0.0370	148	0
2	7.1	0.15	0.05	0.0971	0.0324	236	0
3	10.1	0.30	0.08	0.0960	0.0256	307	-0.01
4	12.6	0.45	0.11	0.0925	0.0226	379	-0.02
5	15.1	0.70	0.16	0.1002	0.0229	442	-0.03
6	17.3	0.90	0.22	0.0981	0.0240	508	-0.04
7	19.8	1.39	0.39	0.1157	0.0325	600	-0.05

Table 12: Performance evaluation for AOA 18°

S.No	Velocity (m/s)	Lift (N)	Drag (N)	Coefficient of Lift (N)	Coefficient of Drag	Speed Rpm	Side Shear
1	4.2	0.04	0.02	0.0740	0.0370	135	0.01
2	7.1	0.14	0.07	0.0906	0.0453	240	0.01
3	10.1	0.30	0.14	0.0960	0.0448	330	0
4	12.6	0.45	0.21	0.0925	0.0432	405	0
5	15.1	0.68	0.32	0.0973	0.0458	481	-0.01
6	17.3	0.85	0.41	0.0927	0.0447	545	-0.02
7	19.8	1.13	0.56	0.0941	0.0446	625	-0.02
8	21.1	1.32	0.66	0.0968	0.0484	675	-0.03
9	23.2	1.60	0.81	0.0970	0.0491	740	-0.05

III. RESULTS AND DISCUSSIONS

A. Effect of PLA (+)material

Based on the simulation results and wind tunnel results, graphs are plotted for coefficient of lift versus angle of attack (α) and coefficient of drag versus angle of attack for both materials. Figure 11, figure 12 and figure 13 shows the variation of lift and drag versus angle of attack at different speeds for PLA (+) and ABS material.

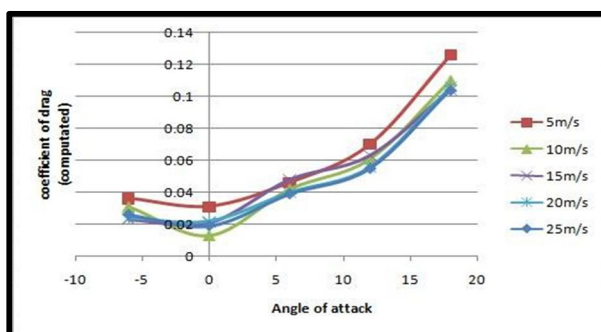


Figure 11(a): C_D (computed) versus α

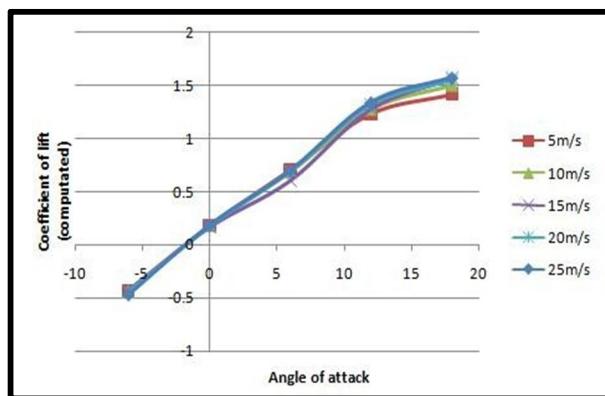


Figure 11(b): C_L (computed) versus α

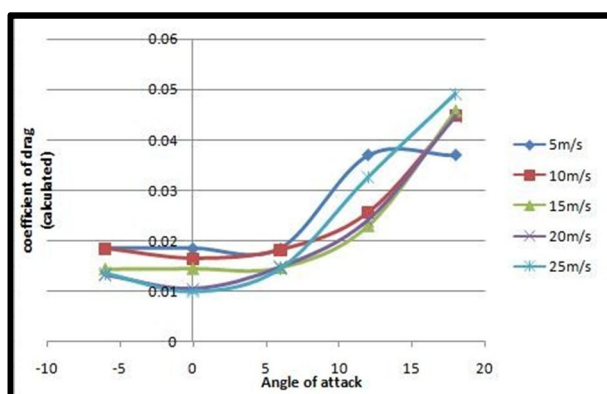


Figure 12(a):: C_D (calculated) versus α

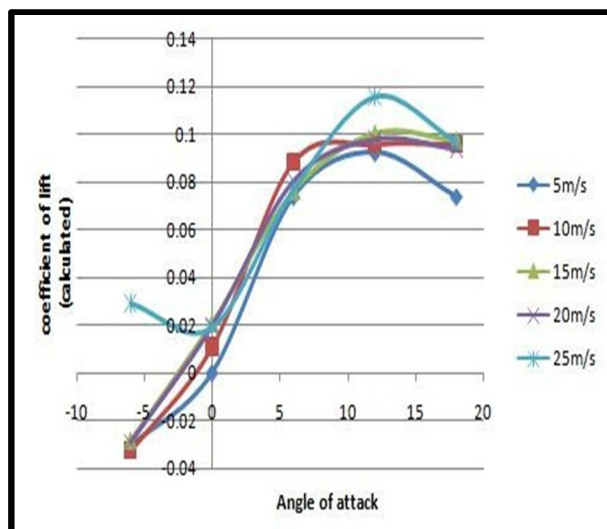


Figure 12(b): C_L (calculated) versus α

There is a considerable difference in the values for the lift and drag coefficients obtained from experimental and simulation methods, one of the possible reasons leading to this difference could be the intensity of turbulence (20-25%) that is present in the wind tunnel, while the turbulence intensity is considered to be around 5% for the simulation.

B. Effect of ABS Material

The coefficient of drag and lift versus angle of attack for different variations in speed are shown in the figure given below.

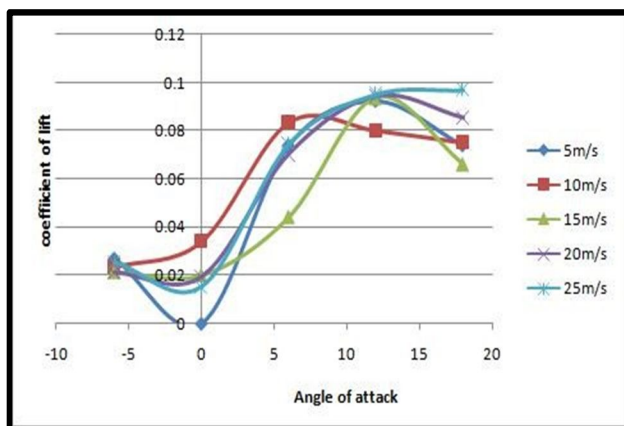


Figure 13(a): C_D for ABS aerofoil

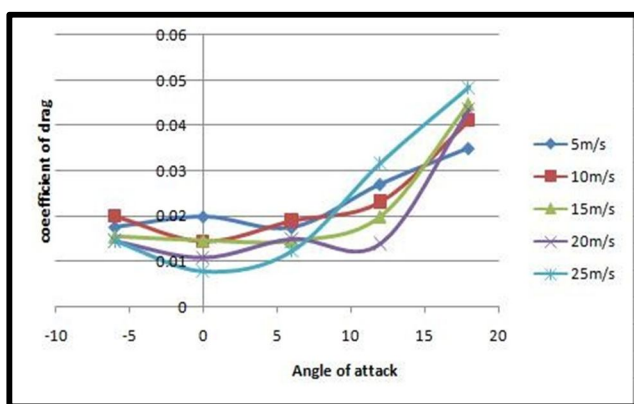


Figure 13(b): C_L for ABS aerofoil

C. Surface Roughness

The reason for considerable difference between results obtained for ABS and PLA (+) is surface roughness. This is to be taken into consideration for the aerodynamic performance of aerofoil.

Ra is calculated as the Roughness Average of surfaces measured by microscopic peaks and valleys when seen using scanning electron microscope. The results obtained are shown in the table 13. Measurements were taken along the span and chord length. It has been observed during the evaluation that chord-wise, roughness measurements were not possible due to excessive irregularities of the surface in case of FDM process. It has been observed that the surface roughness in high-grade PLA material was low when compared to the roughness that has been observed in previously built aerofoil using ABS or standard PLA material.

This is one of the great advantages of preferring high heat grade PLA (PLA+) material over the standard PLA or ABS material.

Table 13: Surface roughness measurement

Choice of Material	Surface Roughness	Process of Fabrication	Coefficient of lift(max)	Coefficient of Drag(max)
PLA(+)	$18 \times 10^{-6} \text{ m}$	FDM	0.115 (12° and 25m/s)	0.048 (18° and 25m/s)
ABS	$20 \times 10^{-6} \text{ m}$	FDM	0.09 (18° and 25m/s)	0.048 (18° and 25m/s)

D. Dimensional Accuracy

In order to check the accuracy of the printed model with respect to CAD design, dimensions have been verified along the wingspan, chord and mean thickness. Measurements were taken with standard caliper of accuracy 0.01mm. Table 14 shows the average results of measurements with relative difference (with respect to CAD design).

Table 14: Shows the average results of measurements and errors percentage after additive manufacturing

Material	B_i	ΔB_i	C_i	ΔC_i	t_i	Δt_i
PLA(+)	249.60	-0.16 %	200.38	0.189%	44.80	-0.446%
ABS	249	-0.40%	198.17	-0.5%	45.7	1.53%

All units are in mm

B denotes Wing span length, C denotes chord length, t denotes thickness

E. Discussions

From Figures 11 and 12, we see that at AOA of 12° and $v = 25\text{m/s}$, the aerofoil with PLA (+) attains the maximum coefficient of lift and at AOA of 18° and $v = 25\text{m/s}$ the aerofoil attains the maximum coefficient of drag. The value for C_L max for aerofoil with PLA (+) is 0.115 and C_D max is 0.048. Similarly the C_L and C_D max for the aerofoil with ABS material is attained at AOA 18° and 25/s. The C_L max for aerofoil with ABS is 0.09. The percentage increase in C_L by using the PLA (+) aerofoil when compared with ABS aerofoil is 27.7%. It can be seen from the graphs, the figures 11(b) and 12(a) that with the increase in the skin friction and the lift coefficient decreases, the surface roughness is seen to delay the stall angle and also increase the lift in the stall region.

FDM printout is characterized by very high roughness value which is obvious due to manufacturing process nature. The surface roughness of PLA(+) material is lower than that of ABS material. Also it has been observed that the dimensional accuracy of PLA(+) material is better compared to ABS material. This is because of high surface finish properties of PLA(+) after printing. Krzysztof OLASEK et al. performed an experiment for the surface property evaluation of ABS aerofoil using FDM technique. Also it can be seen that excessive irregularities of the surface influencing significantly serial measurement because of which measurement of chord-wise and span-wise surface roughness was difficult [15].

IV. CONCLUSIONS

The dimensional accuracy of PLA (+) material has close tolerances and better when compared to ABS material. Surface roughness was evaluated and it has been observed that PLA (+) material showed lesser values compared to ABS material. The drag developed in ABS aerofoil would be more due to high surface roughness whereas it can be minimized when we go for high heat grade PLA material where the surface properties are far better and accurate.

Application of 3d printed high heat grade PLA material space applications where minimal surface friction is desirable with minimum payload weight. This type of 3d printed 6 series NACA aerofoil can be utilized in building drones, air surveillance vehicles, UAV's, because of its light weighted structure and considerable low value of drag under usual operating conditions. Also its application can also be found in Nano-airborne applications like Nano-drones.

REFERENCES

- [1] Guo N, Leu M C. Additive manufacturing: Technology, applications and research needs. *Frontiers of Mechanical Engineering* 2013; 8(3): 215–24
- [2] Mudge RP, Wald N R. Laser engineered net shaping advances additive manufacturing and repair. *Welding Journal-New York*, 2007,86(1):44–48
- [3] Hedges M, Calder N. Near net shape rapid manufacture & repair by LENS. In: *Cost Effective*
- [4] *Manufacture via Net-shape Processing*. Neuilly-sur-Seine, France, 2006, 13–14
- [5] Horn TJ, Harrysson OLA. Overview of current additive manufacturing technologies and selected applications. *Science Progress* 2012;95(3):255–282.
- [6] Jason C, Sean R, David D, Rishi G, Luke D, Josh A, Andie , Alex ,Douglas ,Calvin Kroese, Peter Experimental Characterization of the Mechanical Properties of 3D-Printed ABS and Polycarbonate Parts. *Rapid Prototyping Journal*, 23(4):811-824
- [7] Kruth J, Leu MC, Nakagawa T. Progress in additive manufacturing and Rapid Prototyping. *CIRP Annals- Manufacturing Technology* 1998;47(2):525–540.
- [8] M. Krishna, S. Raghav, T. Panneerselvam and S. Raghuraman, "Review On Properties Of Aerospace Materials Through Additive Manufacturing" *International Journal of Modern Trends in Engineering and Research*, 2017, 4(3), 120-137.
- [9] Ning F, Cong W, Qiu J, Wei J, Wang S. Additive manufacturing of carbon fiber reinforced thermoplastic composites using fused deposition modeling. *Composites Part B: Engineering* 2015; 80: 369–378.



- [10] Bade L, Hackney PM, Shyha I, Birkett M. Investigation into the development of an additive manufacturing technique for the production of Fibre composite products. *Procedia Engineering* 2015; 132: 86–93.
- [11] Tekinalp HL, Kunc V, Velez-Garcia GM, Duty CE, Love LJ, Naskar AK, Blue CA, Ozcan S. Highly oriented carbon fiber–polymer composites via additive manufacturing. *Composites Science and Technology* 2014; 105:144–150.
- [12] Njuguna J, Pielichowski K. Polymer Nanocomposites for aerospace applications: Properties. *Advanced Engineering Materials* 2003; 5(11): 769–778.
- [13] Ben W, Joshuwa M. The effects of PLA color on material properties of 3-D printed components. *Additive Manufacturing journal*. 2015.8.110-116.
- [14] Anderson, Jr., J.D., “Aircraft Performance and Design”, McGraw-Hill, 1999
- [15] Krzysztof O, Piotr W, Wind tunnel experimental investigations of a diffuser augmented wind turbine model, *International Journal of Numerical Methods for Heat & Fluid Flow*, 2016, 26 (7), 2033-2047.



10.22214/IJRASET



45.98



IMPACT FACTOR:
7.129



IMPACT FACTOR:
7.429



INTERNATIONAL JOURNAL FOR RESEARCH

IN APPLIED SCIENCE & ENGINEERING TECHNOLOGY

Call : 08813907089  (24*7 Support on Whatsapp)